Effects of NO_x and VOCs from Five Emission Sources on Summer Surface O_3 over the Beijing–Tianjin–Hebei Region

QU Yu[1], AN Junling[*1], LI Jian[1], CHEN Yong[1], LI Ying[1], LIU Xingang[2,3], and HU Min[3]

[1]*State Key Laboratory of Atmospheric Boundary Layer Physics and Atmospheric Chemistry,*
Institute of Atmospheric Physics, Chinese Academy of Sciences, Beijing 100029
[2]*State Key Laboratory of Water Environment Simulation, School of Environment,*
Beijing Normal University, Beijing 100875
[3]*State Key Joint Laboratory of Environment Simulation and Pollution Control,*
College of Environmental Sciences and Engineering, Peking University, Beijing 100871

ABSTRACT

The impacts of emissions from industry, power plant, transportation, residential, and biogenic sources on daily maximum surface ozone (O_{3DM}) over the Beijing–Tianjin–Hebei (BTH) region in North China in the summer of 2007 were examined in a modeling study. The modeling system consisted of the Weather Research and Forecasting (WRF) model and the photochemical dispersion model, CAMx. The factor separation technique (FST) was used to quantify the effect of individual emission source types and the synergistic interactions among two or more types. Additionally, the effectiveness of emission reduction scenarios was explored. The industry, power plant, and transportation emission source types were found to be the most important in terms of their individual effects on O_{3DM}. The key contributor to high surface O_3 was power plant emissions, with a peak individual effect of 40 ppbv in the southwestern BTH area. The individual effect from the biogenic emission category was quite low. The synergistic effects from the combinations of each pair of anthropogenic emission types suppressed O_3 formation, while the synergistic effects for combinations of three were favorable for O_3 formation when the industrial and power plant emission source types coexisted. The quadruple synergistic effects were positive only with the combination of power plant, transportation, residential, and biogenic sources, while the quintuple synergistic effect showed only minor impacts on O_{3DM} concentrations. A 30% reduction in industrial and transportation sources produced the most effective impacts on O_3 concentrations, with a maximum decrease of 20 ppbv. These results suggested that the synergistic impacts among emission source types should be considered when formulating emission control strategies for O_3 reduction.

Key words: O_3, CAMx model, synergistic effect, factor separation technique, emission source

1. Introduction

The Beijing–Tianjin–Hebei (BTH) region has become a large city cluster in North China due to its rapid economic expansion and industrial development (Chan and Yao, 2008). This expansion has resulted in tremendous increases in emissions of air pollutants, of which elevated surface O_3 pollution is of significant concern. High surface O_3 concentrations have adverse impacts on human health and ecosystems, and moreover have a greenhouse effect on the tropospheric atmosphere (NARSTO, 2000; IPCC, 2001; WHO, 2004). The tropospheric O_3 is not emitted directly into the air; rather, it is formed through a complex series of reactions between nitrogen oxides (NO_x) and volatile organic compounds (VOCs) under favorable meteorological conditions such as strong sunlight and high temperature. The local emission sources of NO_x and VOCs include industrial, power plant, transportation, residential, and biogenic sources. Examining the relative importance of NO_x and VOC emissions from these source sectors is useful for studying O_3 pollution and developing mitigation strategies.

Identifying the sources of elevated ground-level O_3 concentrations is important and has attracted much attention. Vehicle exhaust emissions within Beijing have been reported to be the predominant contributor to O_3 formation in both urban and rural areas (Liu et al., 2008; Yuan et al., 2009; Shao et al., 2009, 2011; Cai and Xie, 2011; An et al., 2012a). Zhang et al. (2011) found that NO_x has shown an increasing trend in Beijing since the 1980s, and the cause of general air pollution

---

* Corresponding author: AN Junling
  Email: anjl@mail.iap.ac.cn

has changed to a mix of traffic exhaust emissions and coal burning-related pollution. O$_3$ pollution results from emissions of NO$_x$ and VOCs from local and regional areas (Jiang and Ma, 2006; Streets et al., 2007; Wang et al., 2009a; Wu et al., 2011). Wang et al. (2010b) found that regional pollution sources contributed >34%–88% to the peak O$_3$ concentrations at urban sites in Beijing when the air masses were from the southeast–south–southwest sector. These studies emphasize NO$_x$-O$_3$ related air pollution problems in the BTH region. In "one atmosphere", the related photochemical reactions between NO$_x$ and VOCs not only occur within the same emission sources but also among different emission sources. However, few studies have evaluated the mutual effect of various emission sources on surface O$_3$. That is, the effect produced by the synergies among emission sources. From the strategy formulation and emission control perspective, information regarding the individual and mutual effects of various emission sources is quite valuable.

Guenther et al. (1995) demonstrated that biogenic emissions of VOCs accounted for more than 90% of global VOC emissions. An increasing number of studies about biogenic emissions in the BTH region are being carried out in response to the significant effects on O$_3$. In the past, biogenic VOCs were thought to play a minor role in O$_3$ formation in Beijing because biogenic VOCs only accounted for a small fraction of the VOC emissions inventory (Shao et al., 2000; Wang and Li, 2002). With the goal of increasing the coverage of green space in Beijing by up to 40% [The United Nations Environment Program (UNEP), 2009] from 2001, the proportion in 2006 increased by 42.5% of the total urban area (Beijing Bureau of Statistics, 2007). Emissions from biogenic sources have been an important source of VOCs in the BTH region (Han et al., 2005; Duan et al., 2008; Yuan et al., 2009; An et al., 2012a). Song et al. (2007) found the role of isoprene, an indicator of biogenic emissions, in O$_3$ formation in Beijing to be comparable to that of anthropogenic sources. Isoprene has been shown to account for 3% of the total O$_3$ formation potential at an urban site in Beijing (Duan et al., 2008), whereas biogenic emissions have been shown to account for 12% of the total O$_3$ formation potential at a rural site in Beijing (Yuan et al., 2009). Thus, it is essential to understand the effects of biogenic emissions in Beijing and its surrounding areas to design effective O$_3$ control measures.

Sensitivity analysis is traditionally used to measure the model output response to emission changes. The "brute-force" approach has been widely utilized to evaluate O$_3$ control measures because it is intuitively easy to explain the source–receptor relations (Guttikunda et al., 2005; Tang et al., 2010; Xing et al., 2011; Gao and Zhang, 2012). In this study, the factor separation technique (FST) of Stein and Alpert (1993), based on multi-"brute force" model simulations, was used to build response relationships between O$_3$ concentrations and O$_3$-precursor sources. There are two major advantages of the FST. First, it characterizes the nonlinear photochemical impacts on O$_3$ by designed experiments via solving a series of linear equations. Second, the FST allows

us to isolate the individual and mutual impacts of two or more factors of interest, e.g., emissions from a variety of sources. Several studies have been conducted to analyze emission effects on O$_3$ formation using the FST. For example, the mutual effects based on specific species like biogenic VOCs and anthropogenic NO$_x$ were investigated by McKeen et al. (1991), Thunis and Cuvelier (2000), Qu and An (2009) and Qu et al. (2009, 2013); the mutual effects based on specific sources, e.g., biogenic and anthropogenic sources (Tao et al., 2003), area, mobile, and point sources (Tao et al., 2005), industry and transportation sources (Weinroth et al., 2008) have also been investigated. However, the effects of various sources— namely, industry, power plant, transportation, residential, and biogenic sources—remain poorly characterized.

The remainder of the paper is organized as follows. The model configuration is described in section 2. The simulation scenarios are presented in section 3. The WRF and CAMx models are evaluated in section 4. The impacts of variable emissions on surface O$_3$ are discussed in section 5. The results from 26 reduction scenarios are evaluated in section 6. And finally, conclusions are drawn in section 7.

2. Model configuration

2.1. *WRF model*

The Advanced Weather Research and Forecasting (WRF-ARW) model, version 3.3, was selected to calculate the off-line meteorological fields for the regional air quality simulations. This version is a non-hydrostatic mesoscale weather modeling system and is flexible for the application of horizontal and vertical resolutions and parameterization schemes. The domains are represented in Fig. 1: the coarsest domain covers almost all of East Asia with a resolution of 81 km, and two nested domains have a horizontal resolution of 27 and 9 km, respectively. The BTH region falls within the finest domain. The vertical layers are from the surface to 100 hPa using a terrain-following sigma-pressure coordinate system collapsed into 18 levels, of which six layers are below 850 hPa (the first model layer is ∼ 50 m above the ground). Two-way nesting was applied because it has been found to yield more accurate results (Harris and Durran, 2010). The Final Analysis (FNL) data from the National Centers for Environmental Prediction (NCEP) were employed as the initial and boundary meteorological conditions. To reduce the uncertainty of the simulation of wind, temperature, and water vapor in the planetary boundary layer, the four dimensional data assimilation (FDDA) was activated to nudge the simulations to the NCEP reanalysis data every six hours. Twenty-four land use types from the United States Geological Survey (USGS) were utilized. The physical options adopted in our study included: the Kain–Fritsch cumulus parameterization scheme (Kain and Fritsch, 1993); the Rapid Radiative Transfer Model (RRTM) scheme (Mlawer et al., 1997) for longwave radiation; the Dudhia scheme (Dudhia, 1989) for shortwave radiation; the medium range forecast (MRF) scheme (Hong and Pan, 1986) for planetary boundary layer; and the five-layer
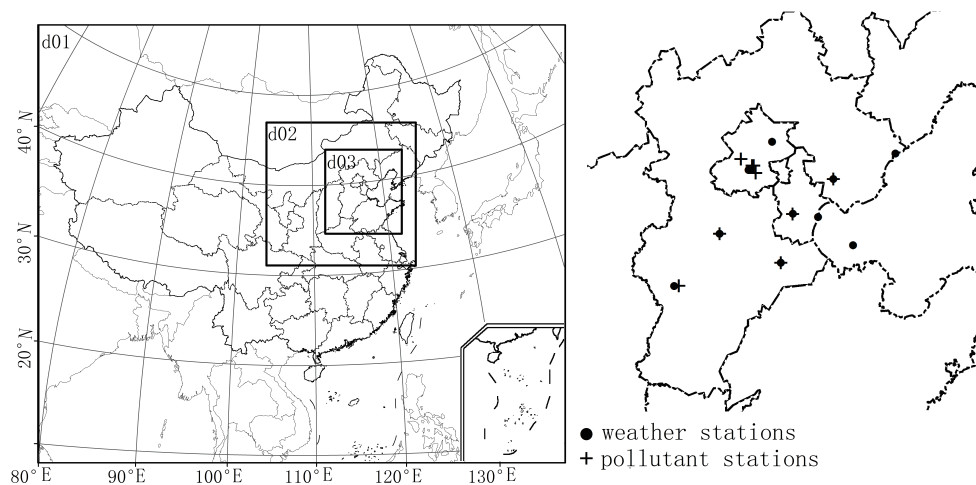
Fig. 1. Domains used and the distribution of observation stations. Black dots denote the 10 routine stations in the BTH region from the CMA; black plus signs denote the nine monitoring stations in the BTH region from the BTH Atmospheric Environment Monitoring Network. YF, AYC, LTH, BJ, BJT, MY, TJ, TJT, TG, TJA, QHD, TS, BD, SJZ, and CZ stand for Yangfang, Aoyuncun, Longtanhu, Beijing, Beijing meteorological tower, Miyun, Tianjin, Tianjin meteorological tower, Tanggu, platform Tianjin A, Qinhuangdao, Tangshan, Baoding, Shijiazhuang, and Cangzhou, respectively.

thermal diffusion land surface scheme.

2.2. *CAMx model*

The comprehensive air quality model with extensions (CAMx), version 5.4 (ENVIRON, 2011), is a nested three-dimensional Eulerian photochemical dispersion model and has been employed extensively throughout the U.S. since 1996. In view of its flexibility in matching the grids of most meteorological models, as well as some notable features such as two-way nesting, multiple chemical mechanism and kinetics solver options, a horizontal advection solver possessing high-order accuracy, and parallel processing, CAMx has increasingly been applied in air pollution research in China (Wang et al., 2009b; Shen et al., 2011; Huang et al., 2012; Wu et al., 2012). In this study, CAMx's map projection and grid structure in both the horizontal and vertical directions were matched to those in WRF to minimize the manipulation of the meteorological data and preserve its credibility to the maximum extent possible (Fig. 1). The initial and lateral chemical boundary conditions were obtained from the Model for Ozone and Related chemical Tracers, version 4 (MOZART-4), with a grid resolution of $2.8° \times 2.8°$ and a frequency of four times each day (Emmons et al., 2010). CAMx was applied with the carbon-bond 2005 (CB05) gas-phase chemistry module (Yarwood et al., 2005) and a revised parameterization for dry deposition of gaseous species scheme (Zhang et al., 2003). It is worth mentioning that the primary photolysis reaction rates were supplied via a large lookup table. The anthropogenic emissions inventory used was based on the 2006 Streets Inventory (Zhang et al., 2009) for East Asia, which was derived from the Transport and Chemical Evolution over the Pacific (TRACE-P) experiment. The power plant sources were assigned to the grids of CAMx, with a height of ~ 100 m above the ground, and this treatment could influence the

simulations adjacent to the power plant sources. To reflect the seasonal dependence of emission sources, we adopted a distinguished ratio of monthly emissions for every species based on the results of Streets et al. (2003) and Zhang et al. (2009). The temporal distribution of transportation sources, derived from the average time intensity of the traffic flow in urban areas (Hao et al., 2000), was characterized by accounting for two rush hours during the day. The biogenic emissions were computed using the Model of Emissions of Gases and Aerosols from Nature (MEGAN; Guenther et al., 2006).

The simulated period was 29 July to 31 August 2007, including three days of spin-up. For both meteorological factors and chemical concentrations, an hourly output frequency was used.

3. Methodology

Once the major O_3 sources including industry (I), power plant (E), transportation (M), residential (C) and biogenic (B) sources were identified, the next step was to determine which source had the strongest impact on the formation of surface O_3.

The FST is a method well-suited to isolating the effects from processes that are linked in a nonlinear way and has been used to quantitatively determine source effects. To evaluate the effects of the five emission sources, 2^5 simulations were performed by WRF-CAMx, as presented in Table 1. The parameter $f_{123\cdots5}$ (f_{IEMCB}) denotes the control run, which considered all five emission sources. Similarly, f denotes the simulation result excluding the five emission sources; the parameter f_i (f_I, f_E, f_M, f_C, f_B) denotes the five simulation results when only one emission source was included in each run; f_{ij} ($f_{\text{IE}}, f_{\text{IM}}, f_{\text{IC}}, f_{\text{IB}}, f_{\text{EM}}, f_{\text{EC}}, f_{\text{EB}}, f_{\text{MC}}, f_{\text{MB}}, f_{\text{CB}}$) denotes the 10 simulation results when two sources

Table 1. Sensitivity scenarios used for the FST[a].

Scenario description	Model results notation[b]
Control run	f_{IEMCB}
No emission	f_0
One emission	f_I, f_E, f_M, f_C, f_B
Two emissions	$f_{IE}, f_{IM}, f_{IC}, f_{IB}, f_{EM},$
	$f_{EC}, f_{EB}, f_{MC}, f_{MB}, f_{CB}$
Three emissions	$f_{IEM}, f_{IEC}, f_{IEB}, f_{IMC}, f_{IMB},$
	$f_{ICB}, f_{EMC}, f_{EMB}, f_{ECB}, f_{MCB}$
Four emissions	$f_{IEMC}, f_{IEMB}, f_{IECB}, f_{IMCB}, f_{EMCB}$

[a]All runs had the same set up as the control run, except for the emission changes listed and conducted from the coarse domain to the finest domain. [b]I, E, M, C, B refer to industry, power plant, transportation, residential and biogenic sources, respectively.

were used in each run; and f_{ijk} ($f_{IEM}, f_{IEC}, f_{IEB}, f_{IMC}, f_{IMB},$ $f_{ICB}, f_{EMC}, f_{EMB}, f_{ECB}, f_{MCB}$) denotes the 10 simulation results when three sources were included in each run. Using f' to denote the individual and synergistic effects of the five emission sources, we have five individual effects (f'_i), ten double interactions (f'_{ij}), ten triple interactions (f'_{ijk}), five quadruple interactions, and one quintuple interaction ($f'_{123\cdots5}$). f' can be calculated by:

$$f_0 = f'_0 + 0\,, \tag{1}$$

$$f_i = f'_i + f'_0\,, \tag{2}$$

$$f_{ij} = f'_{ij} + f'_i + f'_j + f'_0\,, \tag{3}$$

$$f_{ijk} = f'_{ijk} + f'_i + f'_j + f'_k + f'_{ij} + f'_{ik} + f'_{jk} + f'_0\,, \tag{4}$$

$$\cdots\cdots$$

$$f_{123\cdots5} = f'_{123\cdots5} + \sum_{i=1}^{5} f'_i + \sum_{i,j=1,2}^{5-1,5} f'_{ij} +$$
$$\sum_{i,j,k=1,2}^{5-2,5-1,5} f'_{ijk} + \cdots + f'_0\,, \tag{5}$$

where i, j, k represent one of the factors I, E, M, C and B, depending on the sensitivity scenarios shown in Table 1.

f is the background run, representing the impact of initial and boundary chemical fields on O$_3$ formation. The individual effect (f'_i) represents an individual emission source contributing to O$_3$ formation, whereas the multiple interaction ($f'_{ij}, f'_{ijk}, f'_{123\cdots5}$) reflects the nonlinear interaction among two or more emission sources on O$_3$ formation.

In this study, we focused on the effect of different emission scenarios on O$_{3DM}$ concentrations. The O$_{3DM}$ concentrations in each grid cell of the first model layer were taken from the control run model results, f_{IEMCB}, and the corresponding time of the O$_{3DM}$ concentrations was recorded. The O$_3$ concentrations from the other 31 sensitivity scenarios in each surface grid cell at the previous recorded time were selected. The individual and synergistic effects could be computed by solving Eqs. (1)–(5).

4. Model evaluation

4.1. *Comparison of simulations and observations of meteorological factors*

The WRF simulations were assessed against surface hourly meteorological observations at 10 routine stations over the BTH region (Fig. 1, right) from the China Meteorological Administration (CMA). Meteorological variables, i.e., air pressure, temperature, relative humidity (RH) at the first model layer, as well as wind speed and direction at 10 m, were extracted from the grid cell at the site located in the finest domain with a horizontal resolution of 9 km.

The hourly statistical results at the 10 stations are shown in Table 2. Air pressure and temperature were reproduced well by the WRF model, with correlation coefficients of 0.91 and 0.86, respectively, and the deviations between the simulations and observations were within the range of −1% and 6% for NMB (normalized mean bias) and NME (normalized mean error). Simulations of RH were also good, with a correlation coefficient of 0.74 and RMSE (root-mean-square error) of 19.67%. The simulated wind speeds were higher than observed, but still reasonable. These results were comparable to those of Misenis and Zhang (2010) and Zhang et al. (2012). For wind direction, the simulations were not as good a reflection of observations as was the case for wind speed, air temperature and pressure. This is a common feature of all meteorological models, and further improvements are expected in the future.

4.2. *Comparison of simulations and observations of O$_3$ and NO$_x$*

Observed concentrations of O$_3$ and NO$_x$ at nine monitoring stations in the BTH region (Fig. 1, right) were obtained from the BTH Atmospheric Environment Monitoring Network, established by the Institute of Atmospheric Physics,

Table 2. Statistics for the hourly WRF simulations of air pressure, temperature, RH, wind speed and direction in August of 2007.

	Pressure (Pa)	Temperature (°C)	RH (%)	Wind speed (m s^{-1})	Wind direction (°)
R	0.91	0.86	0.74	0.51	0.32
MBE	−315.49	0.16	−15.87	0.12	6.65
RMSE	430.90	1.86	19.67	1.35	110.43
NMB (%)	−0.31	0.62	21.76	6.04	4.13
NME (%)	0.35	5.40	22.63	49.98	50.94

R, correlation coefficient; MBE, mean bias error; RMSE, root-mean-square error; NMB, normalized mean bias; NME, normalized mean error.

Table 3. Statistics for the hourly CAMx simulations of O_3 in the BTH region in August of 2007. O_3 simulated concentrations at nine stations of the BTH region were extracted from the finest domain with a horizontal resolution of 9 km.

		N	C_{model} (ppbv)	C_{obs} (ppbv)	R	MBE (ppbv)	RMSE (ppbv)	NMB (%)	NME (%)
Beijing	Yangfang	405	64.46	54.72	0.80	15.33	28.03	29.60	41.71
	Beijing tower	442	64.05	35.06	0.76	25.04	35.28	70.78	79.11
	Aoyuncun	371	65.37	46.52	0.76	20.05	33.12	40.97	54.54
	Longtanhu	433	62.42	51.03	0.81	9.30	26.51	18.45	40.36
Hebei	Baoding	522	71.20	46.35	0.77	23.42	32.08	50.27	55.59
	Cangzhou	462	71.67	45.14	0.71	24.03	33.32	53.46	60.74
	Shijiazhuang	404	72.50	46.97	0.63	30.48	43.29	72.37	83.49
	Tangshan	464	61.39	33.92	0.73	24.94	33.12	69.93	74.84
Tianjin	Tianjin tower	374	52.31	47.36	0.77	10.74	29.40	26.08	58.53

Chinese Academy of Sciences (Xin et al., 2010; Tang et al., 2012). Large correlation coefficients (0.63–0.81) were calculated for all nine stations (Table 3), indicating that the CAMx model was able to accurately reproduce the temporal variability of the hourly surface O_3 concentrations. Nevertheless, the O_3 concentrations at the nine stations were in fact overestimated. This would have been due mainly to the inadequate area-weighted apportionment of emission sources from coarse to fine grids used in the CAMx model (An et al., 2012b) and the gas chemical mechanism overestimating O_3 peaks during the day and underestimating O_3 titration at night.

The O_{3DM} and daily mean NO_x at the nine stations were averaged according to each of the three political regions, i.e., the provinces of Beijing, Tianjin, and Hebei. The time series of the comparison between observed and simulated concentrations of O_3 and NO_x are shown in Fig. 2. It is impressive that the diurnal variations of the O_3 peak and daily mean NO_x are distinct in the three regions, suggesting that the pollution dynamics were well captured by the CAMx model. The simulated O_3 peaks were comparable with observations, and the simulated and observed daily mean NO_x agreed fairly well in the provinces of Beijing and Hebei. For Tianjin, only one station was available, and a tendency toward NO_x overestimation was found. This could have been associated with the inaccuracy of the emission interpolation (Ma and van Aardenne, 2004). Nevertheless, the overall model performance for O_3 and NO_x was comparable with other CAMx applications (Castell et al., 2011; Shen et al., 2011; Li et al., 2012).

5. Individual and synergistic effects

5.1. *Spatial distributions of the individual effects of the five emission sources*

According to the FST, the individual effects ($f'_I, f'_E, f'_M, f'_C, f'_B$) are the differences between the simulation results when only one emission source is considered, and when all the emissions are excluded [Eq. (2)]. The individual effect reflects the O_3 formation potential of each source. The percentage of the total individual effect of the five sources to O_{3DM}, i.e., $(f'_I + f'_E + f'_M + f'_C + f'_B)/O_{3DM} \times 100\%$, was above 80%
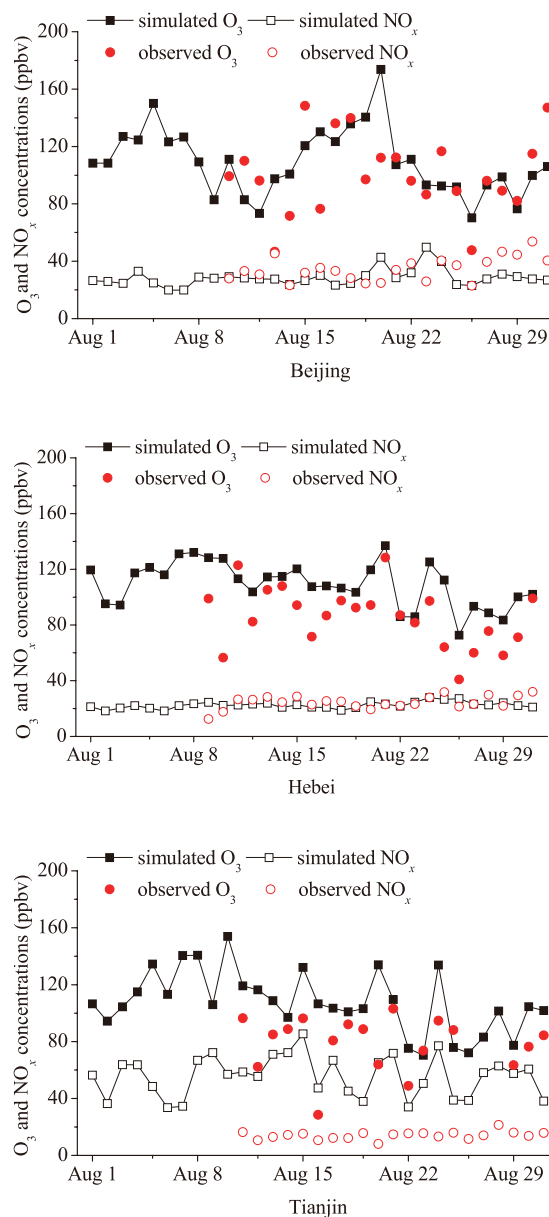
Fig. 2. Variations of simulated (black squares) and observed (red circles) O_{3DM} concentrations (ppbv) in August of 2007.

throughout almost the entire BTH region, and even above 100% in the southwestern areas of Beijing and Hebei (not shown), demonstrating the remarkable individual effects on O_3 formation.

The spatial distribution of the H_2O_2/HNO_3 ratio (see Electronic Supplementary Material; Figs. S1–S5) is often regarded as an index to identify NO_x-limited or VOC-limited regimes in O_3 photochemical production (Wang et al., 2005; He et al., 2010; Peng et al., 2011). The transition value set as 0.4–0.6 was adopted according to field measurements in Beijing in 2008 (He et al., 2010), in which a value of > 0.6 would indicate an NO_x-limited regime, a value of < 0.4, a VOC-limited regime, and otherwise an intermediate regime. The H_2O_2/HNO_3 ratios at the O_{3DM} time of each day were extracted from the five simulations when only one emission source was considered (Table 1: f_I, f_E, f_M, f_C, f_B) and averaged for the month. The ratios were all above 0.6 in the BTH region (Fig. S1), suggesting that the BTH region is an NO_x-limited region. This result does not conflict with previous results reporting the BTH urban area to be VOC-limited (Chou et al., 2009; Wang et al., 2010b; Yang et al., 2011) when all

the source types were considered.

The distributions of the individual effects of each source type are shown in Fig. 3. As can be seen, the monthly average effects of each source type on O_{3DM} were distinct in both space and amplitude. The individual effects of industry, power plants, and transportation sources in the BTH region were above 20 ppbv, much larger than those of residential and biogenic sources. The larger effects (> 30 ppbv) of sources from industry (Fig. 3a) occurred in the southwestern areas of Beijing and Hebei, where a significant amount of industrial NO_x and VOCs are emitted. The most important contributor to high surface O_3 was the power plant source (Fig. 3b); effects above 30 ppbv were found throughout almost the entire BTH region, and the peak effects in southwestern Hebei Province reached 40 ppbv. Compared with the other four emission sources, NO_x emissions from power plants were dominant (Fig. 4b) and played a vital role in the NO_x-limited regimes of O_3 production ($H_2O_2/HNO_3 > 0.6$, Fig. S1b). The total emission amounts of NO_x and VOCs from the transportation source were comparable to those from industry (Fig. 4), but the transportation source was concen-
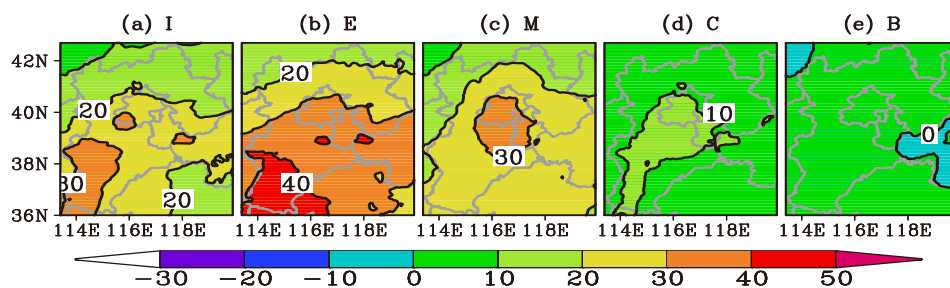
Fig. 3. Monthly average individual effects (ppbv) of the five individual source categories on O_{3DM} concentrations in August of 2007: (a) industry; (b) power plant; (c) transportation; (d) residential; and (e) biogenic.
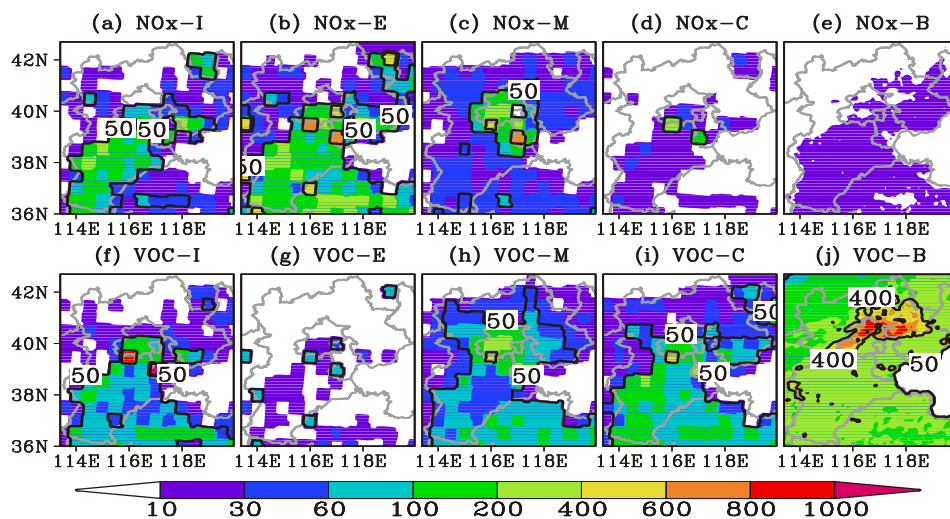
Fig. 4. NO_x and VOC emission rates (ng m⁻² s⁻¹) of the five source categories in August of 2007: (a, f) industry; (b, g) power plant; (c, h) transportation; (d, i) residential; and (e, j) biogenic.

trated in Beijing and Tianjin. As a result, large effects of the transportation source occurred in Beijing and its surrounding areas (Fig. 3c). A residential source effect of above 10 ppbv occurred near Beijing, Tianjin, and southern Hebei (Fig. 3d), which are densely populated areas in the BTH region. Although biogenic VOCs emissions were high, accounting for more than half of total VOC emissions in the BTH region (Fig. 4j), the impacts on surface O_3 were quite low (Fig. 3e). The effects were below 10 ppbv over the entire BTH region. The reason was that the biogenic NO_x emissions were too low to provide enough NO_x for O_3 formation in the NO_x-limited regimes ($H_2O_2/HNO_3 > 0.6$, Fig. S1e).

5.2. Spatial distributions of the synergistic effects of two or more emission sources

In terms of chemical species, the individual effects are the interactions between NO_x and VOCs from the same source type, whereas the synergistic effects are those from different source types. The addition of the paired, triple, quadruple, and quintuple synergistic effects accounted for 20% of the O_{3DM} reductions in most areas of the BTH region, and the negative effects were below -40% in the southwestern areas of Beijing and Hebei, where the individual effects were high. This indicated that the synergistic effects due to the combined effects of NO_x and VOCs from some source types had changed from NO_x-limited regimes to VOC-limited regimes, and sometimes suppressed O_3 formation in comparison with the individual effects. The monthly H_2O_2/HNO_3 ratios (Figs. S2–S5) at the O_{3DM} time were extracted from the simulations that included two or more emission sources (Table 1) to help identify NO_x-or VOC-limited regions, and the results are described below.

5.2.1. Synergistic effects between two sources

From Fig. 5 we can see that the synergistic effects between two emission sources excluding the biogenic source ($f'_{IE}, f'_{IM}, f'_{IC}, f'_{EM}, f'_{EC}, f'_{MC}$) were all negative (Figs. 5a–f), demonstrating that the paired combinations among anthropogenic emissions (industry, power plant, transportation, and residential sources) actually suppressed O_3 formation in the BTH region.

The largest negative effects, with a value of below 30 ppbv (Fig. 5a), were found in southern Beijing, northern Tianjin, and southwestern Hebei, where large NO_x emissions from industrial plants and power plants coexist. The NO_x emissions from transportation were mainly located in Beijing and Tianjin (Fig. 4c), where vehicle volumes are higher. Correspondingly, larger negative synergistic effects (< -20 ppbv) between industry and transportation sources (Fig. 5b), or between power plant and transportation sources (Fig. 5d), were found in these two areas. The common characteristic of the H_2O_2/HNO_3 ratios for the source combinations shown in Figs. 5a, b and d was a value of below 0.4 in the southwestern area of Beijing and Hebei (Figs. S2a, b, and d), representing a VOC-limited chemical regime where NO_x emissions were dominant and a further increase in NO_x would remove radicals and hinder O_3 formation.

The residential NO_x emissions were concentrated in limited areas of Beijing and Tianjin (Fig. 4d), while VOC emissions were relatively high and played an important role in the synergistic effects with the other three anthropogenic emission sources (Figs. 5c, e and f). Higher VOC emissions weaken O_3 formation to a certain extent in a VOC-rich region ($H_2O_2/HNO_3 > 0.6$, Figs. S2c, e, and f) (An et al., 1999; Diem, 2000; Zhu et al., 2006), so the synergistic effects on O_{3DM} were negative.

Positive effects can be seen in the results presented in Figs. 5g–j, when biogenic emissions were considered ($f'_{IB}, f'_{EB}, f'_{MB}, f'_{CB}$). This was because O_3 concentrations typically exhibit a nonlinear response, and the O_3 nonlinearity in a given emission region is mostly dependent on the intensity of NO_x emissions (Lin et al., 1988; Cohan et al., 2005). The greater effects above 10 ppbv were located across almost the entire area of Beijing and northern Tianjin (Fig. 5h), due to large NO_x emissions from power plants and substantial biogenic VOC emissions ($H_2O_2/HNO_3 > 0.6$, Fig. S2h). The synergistic effects involving industry (Fig. 5g) and transportation sources (Fig. 5i) were < 10 ppbv over the entire BTH region and were comparable to those involving residential sources (Fig. 5j), although the NO_x emissions from residential sources were much lower than those from industry and transportation sources. It should be mentioned that the paired synergistic effects with biogenic sources (Figs. 5g, i and j) were not significantly greater than the individual effect of biogenic sources (Fig. 3e). This was because large levels of biogenic VOCs need large levels of NO_x emissions to form more O_3, although NO_x emissions can increase O_3 formation in a NO_x-limited chemical regime ($H_2O_2/HNO_3 > 0.6$, Figs. S2g, i, and j).

5.2.2. Synergistic effects among three or more sources

We also compared the spatial distribution patterns of triple synergistic effects of the five emission sources ($f'_{IEM}, f'_{IEC}, f'_{IMC}, f'_{EMC}, f'_{IEB}, f'_{IMB}, f'_{ICB}, f'_{EMB}, f'_{ECB}, f'_{MCB}$) (Fig. 6). As can be seen, greater effects (> 10 ppbv) were found among industry, power plant, and transportation sources (Fig. 6a); industry, power plant, and residential sources (Fig. 6b); and industry, power plant, and biogenic sources (Fig. 6c). Although the paired synergistic effects between industry and power plant sources were persistently negative throughout the BTH region (Fig. 5a), the addition of any other emission source (transportation, residential, biogenic) led to a transition from negative to positive effects. However, the O_3 increases, caused by the addition of NO_x or VOC emissions from transportation, residential sources and biogenic sources, were distinct among the three synergies. When industry, power plant, and transportation sources or residential sources coexisted (Figs. 6a, b), the O_3 formation was VOC-limited ($H_2O_2/HNO_3 < 0.4$, Figs. S3a and b). High VOC emissions from transportation or residential sources can supply abundant radicals of OH and HO_2 and then lead to NO conversion to NO_2 and O_3 accumulation (Ma et al., 2012). Industrial and power plant sources provide abundant NO_x emissions, which would have led to O_{3DM} increases in the
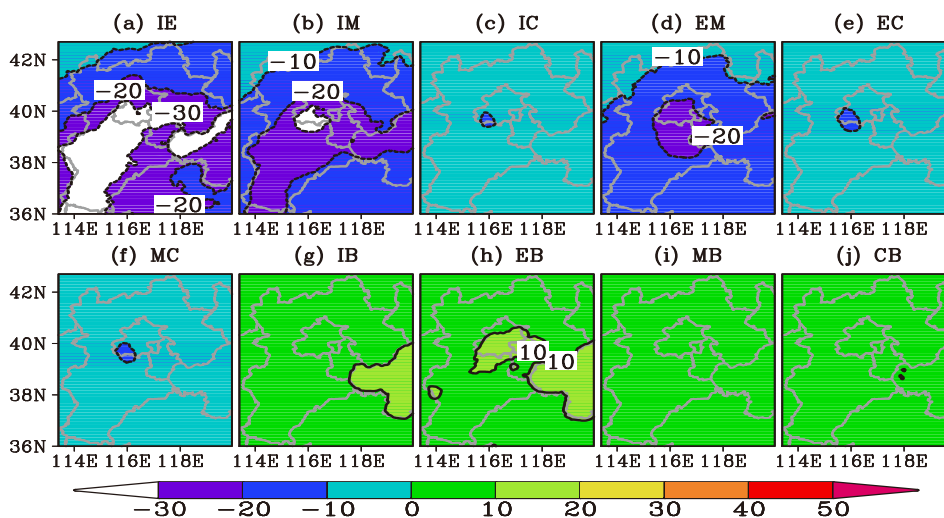
Fig. 5. Monthly average synergistic effects (ppbv) between two sources on O$_{3DM}$ concentrations in August of 2007: (a) industry and power plant; (b) industry and transportation; (c) industry and residential; (d) power plant and transportation; (e) power plant and residential; (f) transportation and residential; (g) industry and biogenic; (h) power plant and biogenic; (i) transportation and biogenic; and (j) residential and biogenic.
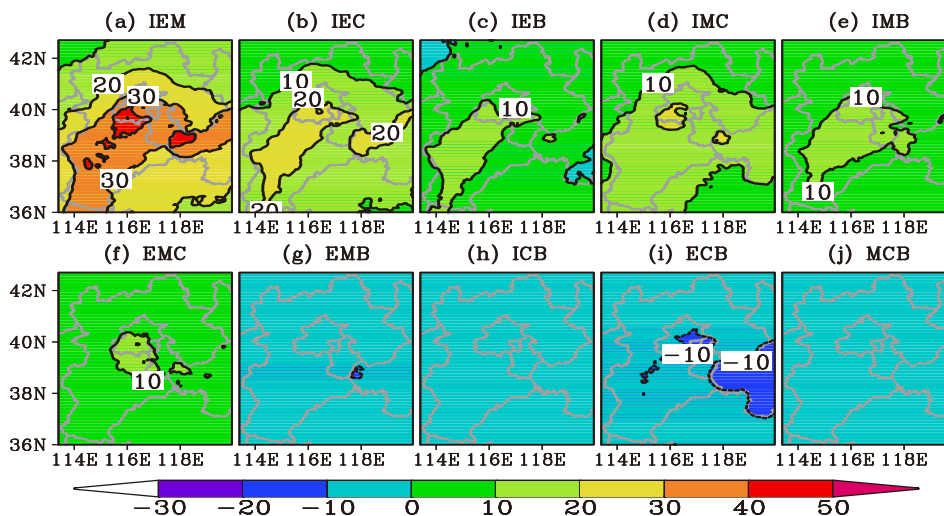
Fig. 6. Monthly average synergistic effects (ppbv) among three sources on O$_{3DM}$ concentrations in August of 2007: (a) industry, power plant, transportation; (b) industry, power plant, residential; (c) industry, power plant, biogenic; (d) industry, transportation, residential; (e) industry, transportation, biogenic; (f) power plant, transportation, residential; (g) power plant, residential, biogenic; (h) industry, residential, biogenic; (i) power plant, transportation, biogenic; (j) transportation, residential, biogenic.

NO$_x$-limited regime (H$_2$O$_2$/HNO$_3$ > 0.6, Fig. S3c) when they interacted with the high biogenic VOC emissions (Fig. 6c).

The effects among industry, transportation, and residential sources (Fig. 6d) or biogenic sources (Fig. 6e) were above 10 ppbv and located in the central and southern areas of the BTH region. NO$_x$ emissions from industry and transportation sources were slightly lower than those from industrial and power plant sources (Fig. 4). Similarly, VOC emissions from residential sources were favorable for O$_{3DM}$ increases

when industry, transportation and residential sources coexisted (Fig. 6d; H$_2$O$_2$/HNO$_3$ < 0.4, Fig. S3d), while NO$_x$ emissions from industry and transportation sources were important for the synergy when biogenic sources were taken into account in O$_3$ formation (Fig. 6e; H$_2$O$_2$/HNO$_3$ > 0.6, Fig. S3e).

Compared with the paired synergistic effects between power plant and transportation sources (Fig. 5d), the triple synergistic effects changed to positive when the residential

sources were included (Fig. 6f), owing to the increase of VOC emissions in the VOC-limited regime ($H_2O_2/HNO_3 < 0.4$, Fig. S3f). The O_{3DM} concentrations due to triple synergistic effects (Fig. 6g) were higher than those due to the paired synergy shown in Fig. 5d, but were still negative when biogenic sources were considered. The fewer NO_x emissions, which are the essential source of O_3 formation, was the main reason, although biogenic VOCs could promote O_{3DM} concentrations in the VOC-limited regime ($H_2O_2/HNO_3 < 0.4$, Fig. S3g).

The synergistic effects among residential, biogenic, and other source combinations were reduced to below zero, as illustrated in Figs. 6h–j, because VOC emissions from residential and biogenic sources were high and a further increase in VOCs would have suppressed O_3 formation in the NO_x-limited regime ($H_2O_2/HNO_3 > 0.6$, Fig. S3h–j).

Figure 7 illustrates the synergistic effects when four emission sources were considered ($f'_{IEMC}, f'_{IEMB}, f'_{IECB}, f'_{IMCB}, f'_{EMCB}$). As can be seen, the common feature was that most of the synergistic effects were reduced to below zero. The industry, power plant, and transportation sources with residential or biogenic sources were negative contributors to O_{3DM} over the entire BTH region (Figs. 7a, b). This was because the total NO_x emissions from industry, power plant, and transportation sources were relatively high among the five emission sources, and more increases in NO_x when the residential or biogenic sources were included would have retarded O_3 formation in the VOC-limited regime ($H_2O_2/HNO_3 < 0.4$, Figs. S4a and b). In contrast, the NO_x emissions from the residential and biogenic sources were low. When these two sources and industry, power plant, or transportation sources were considered, the quadruple synergistic effects in Figs. 7c–e ($H_2O_2/HNO_3 > 0.6$, Figs. S4c–e) tended to increase over most areas of the BTH region, compared with the paired synergy in Figs. 5a, b and d.

Finally, Fig. 8 shows the synergistic effect (f'_{IEMCB}) when five emission sources were included. It can be seen that the quintuple synergistic effects had only minor impacts on O_{3DM} concentrations.

According to the above results, we are able to conclude that industry, power plant and transportation sources are the most important contributors to O_{3DM} in the BTH region, and so the implementation of control strategies among these three anthropogenic emission sources are advisable.

6. Impacts of emission source reduction scenarios on O_{3DM}

To explore the possible impacts of emission reductions on O_{3DM} concentrations within the three source types identified as being the most important contributors, 26 reduction scenarios were considered. The emissions from industry, power plant, and transportation sources in all three domains were reduced by 30% and 80%. Figure 9 shows the differences in the monthly average O_{3DM} concentrations between each of the 26 scenarios and the control run case. When only one emission sector was reduced (Figs. 9a1–f1), the O_3 decreases were < 20 ppbv. Following a 30% reduction, the three source types had minor impacts on O_3 concentrations, with mean values decreased by < 5 ppbv over the entire BTH region. As established above (Fig. 4b), power plant sources were found to play a key role in O_3 formation, and it seems that reducing power plant emissions by 80% would produce the greatest effect on O_3 concentrations. Results showed the impacts to be $\sim$10–20 ppbv throughout Tianjin and southern Hebei (Fig. 9e1).

Compared with the scenarios of only one emission reduction, O_3 concentrations were substantially reduced when two emission source types were simultaneously decreased, due to the synergistic impacts (Figs. 9a2–f2). A 30% reduction in industry and transportation sources showed the most effective impacts on O_3 concentrations, with a maximum decrease of 20 ppbv in Beijing, Tianjin, and southern Hebei (Fig. 9b2), where O_3 pollution is heavy. When two emission sectors were simultaneously reduced by 80%, O_3 concentrations were substantially decreased by $\sim$10–40 ppbv (Figs. 9d2–f2), indicating that a large emission reduction would have a significant effect on O_3 levels. It is noted that the reduction in industry and transportation sources had the least effective impacts on O_3 concentrations (Fig. 9e2), as compared with when the two sources were reduced by 30%
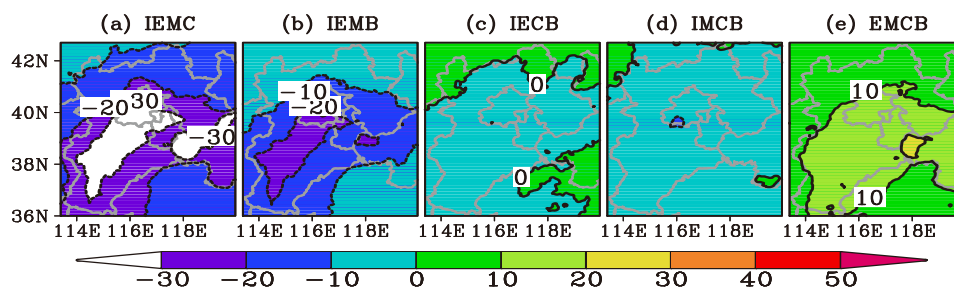
Fig. 7. Monthly average synergistic effects (ppbv) among four sources on O_{3DM} concentrations in August of 2007: (a) industry, power plant, transportation, residential; (b) industry, power plant, transportation, biogenic; (c) industry, power plant, residential, biogenic; (d) industry, transportation, residential, biogenic; and (e) power plant, transportation, residential, biogenic.
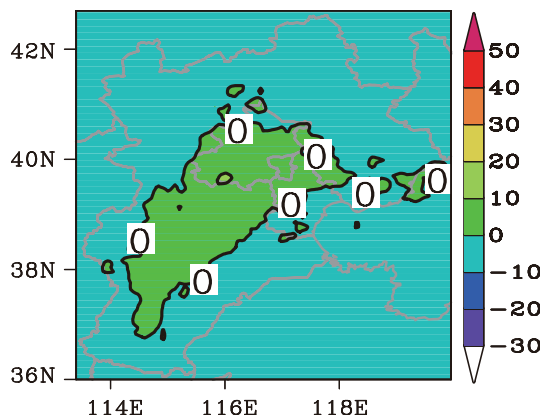
Fig. 8. Monthly average synergistic effects (ppbv) among industry, power plant, transportation, residential, and biogenic sources on O$_{3DM}$ concentrations in August of 2007.

(Figs. 9b2), due to the nonlinear process of O$_3$ formation. A larger decrease in O$_{3DM}$ covered the southern BTH region due to a large reduction in power plant emissions (Figs. 9d2 and f2).

For the 30% and 80% emission reduction combinations between two emissions (Figs. 9a3–f3), impacts of $\sim$ 5–30 ppbv were obtained. The combination of an 80% reduction in power plant emissions and a 30% reduction in transportation emissions (Fig. 9d3) seemed to be the most effective control scenario; the O$_{3DM}$ concentrations in most areas of the BTH region could be reduced by more than 20 ppbv. The combination of a 30% reduction in industrial emissions and an 80% reduction in power plant emissions (Fig. 9a3) indicated a significant impact on O$_3$ concentrations over the southwestern BTH region, where the large cities and large emission sources of Hebei Province are located.

Additional reduction scenarios were performed and showed that a 30% reduction in industrial emissions, an 80% reduction in power plant emissions, and a 30% reduction in transportation emissions, led to the largest decreases of $\sim$ 20–30 ppbv in O$_{3DM}$ (Fig. 9c4), as compared with other emission reduction combinations if only one of the three emission sources was reduced by 80% (Figs. 9a4, b4 and d4). An 80% reduction in industrial emissions and an 80% power plant emissions reduction led to a significant decrease of O$_{3DM}$ across most of the BTH region, with the largest decrease of 40 ppbv occurring in the southern areas of Hebei Province (Fig. 9g4). The largest emission reduction combination is shown in Fig. 9h4; O$_{3DM}$ concentrations were decreased by more than 40 ppbv in Beijing and southwestern Hebei. It should be noted that an 80% reduction in the three emission sources is the strictest strategy of the 26 reduction scenarios, but was found not to be the most effective control measure.

Another feature of the 26 reduction scenarios was that an 80% power plant emission reduction led to an O$_3$ decrease of above 10 ppbv, as illustrated in Figs. 8e1, d2, f2, a3, d3, and c4, showing that larger emission reductions in the power plant source type, along with lower emission reductions in the other two source types, could effectively prevent O$_3$ for-

mation in the southwestern BTH region. A reduction in transportation emissions, highlighted in Fig. 4c for Beijing, could effectively cut down O$_3$ concentrations there (Figs. 9f1, b2, f2, b3, c3, and d3). This finding suggests that O$_3$ pollution control should not only be based on single emission sources, but also take into account several related sources; the synergy owing to different emission sources in local and regional areas may produce more favorable effects in terms of cutting down O$_3$ pollution, which is consistent with the previous findings of Streets et al. (2007), Wang and Xie (2009), Wang et al. (2009b), Wang et al., (2010a), and Yang et al. (2011).

7.   Summary and conclusions

The WRF-CAMx model was employed to simulate summer O$_3$ in 2007 to explore the impacts of industry, power plant, transportation, residential, and biogenic emission sources on daily maximum surface ozone (O$_{3DM}$) in the BTH region. Furthermore, 26 emission reduction scenarios were examined to evaluate the effectiveness of O$_3$ control strategies. The conclusions of the study are as follows:

The individual effect of each source type reflects its O$_3$ formation potential. In terms of monthly averages, the individual effects of each source type to O$_{3DM}$ were distinct in space and amplitude. The individual effects of industry, power plant, and transportation emissions in the BTH region were substantially greater than those from residential and biogenic emissions. The most important contributor was the power plant source, with a peak individual effect of 40 ppbv in the southwestern BTH region. Larger individual effects of the industrial source were found for the southwestern BTH region, whereas larger individual effects of the transportation source were found for Beijing and Tianjin, where NO$_x$ and VOC emissions are high. The biogenic individual effects were very low.

The key characteristic of paired synergistic effects in the BTH region was that a combination of anthropogenic emissions, i.e., industry, power plant, transportation, and residential sources, suppressed O$_3$ formation. Positive effects were found in the paired synergistic effects of anthropogenic NO$_x$ sources with biogenic sources. As for the synergistic effects among three sources, the interactions of industrial and power plant emissions were favorable for O$_3$ formation, although the paired synergistic effects between industry and power plant sources were negative throughout the BTH region. When four emission sources were considered, the synergistic effects were reduced to below zero, except for the combination of power plant, transportation, residential, and biogenic sources. The synergistic effect showed minor impacts on O$_{3DM}$ concentrations when five emission sources were considered.

If only one emission type was reduced, the industry, power plant, and transportation source types had minor impacts on O$_3$ concentrations over the entire BTH region, in terms of a 30% emission reduction. An 80% power plant emission reduction led to the largest O$_3$ decrease of $\sim$10–20
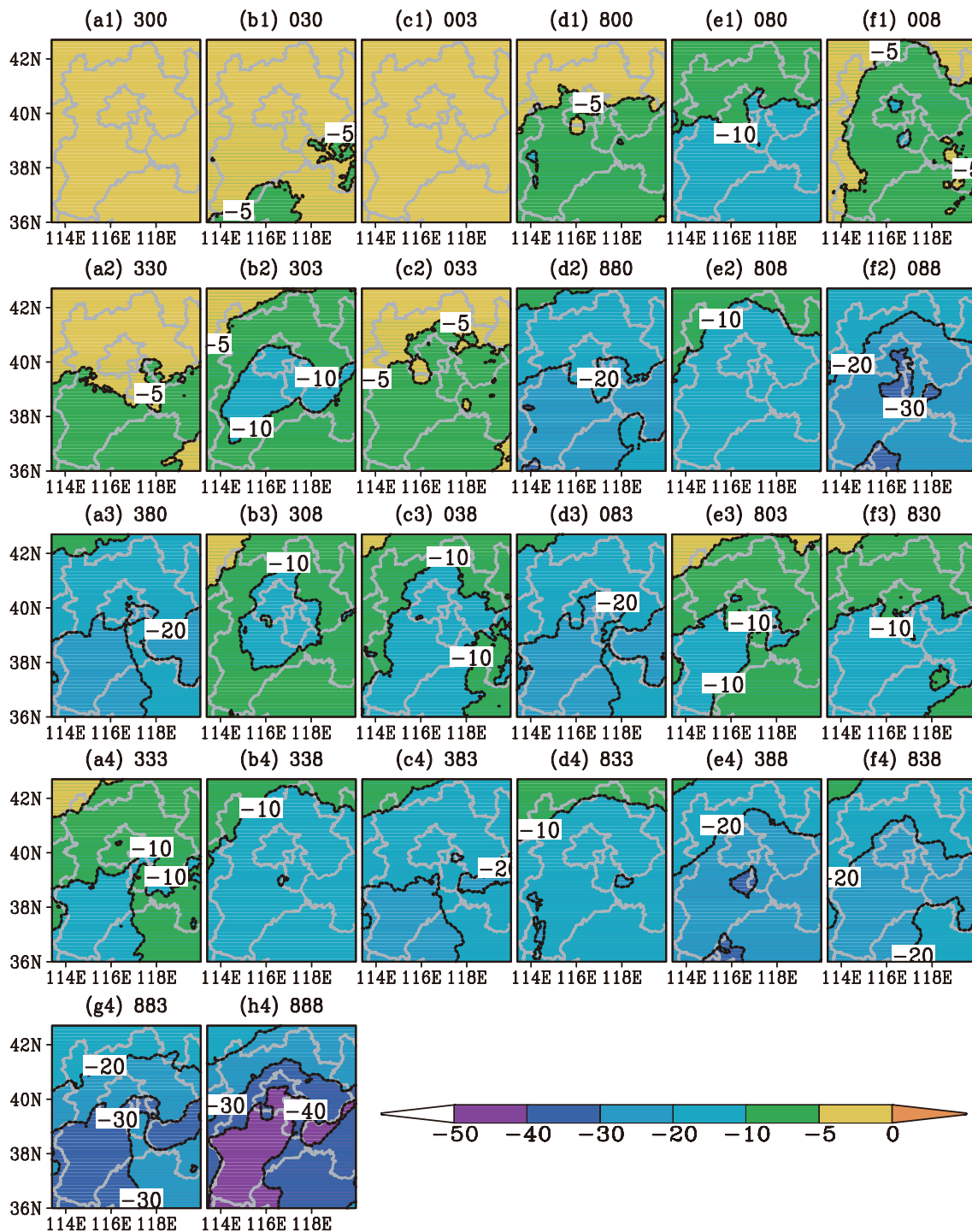
Fig. 9. The differences (ppbv) in monthly average O$_{3DM}$ concentrations between each of 26 emission reduction scenarios and the control run in August of 2007. For example, a combination of 0, 3, and 8 in the title of each panel denotes a reduction of 0% in industrial source emissions, 30% in power plant source emissions, and 80% in transportation source emissions.

ppbv throughout Tianjin and southern Hebei. O$_3$ concentrations were significantly reduced when two or three emission sectors were simultaneously reduced, due to the synergistic impacts. When two emission sectors were simultaneously reduced by 30%, the industry and transportation source reductions had the most effective impacts on O$_3$ concentrations,

with a maximum decrease of 20 ppbv in Beijing, Tianjin, and southern Hebei, where O$_3$ pollution is heavy. For the 30% and 80% emission reduction combinations between two emissions, an 80% emission reduction in power plant sources and a 30% emission reduction in transportation sources were found to be effective for O$_{3DM}$ concentrations across most of

the BTH region, with a maximum O$_3$ decrease of 30 ppbv. When three emission sectors were simultaneously reduced and only one of them was reduced by 80%, a 30% reduction in industrial emissions, an 80% reduction in power plant emissions, and a 30% reduction in transportation emissions produced the greatest impacts on surface O$_3$. An 80% power plant emission reduction along with lower emission reductions in the other two sources led to an O$_3$ decrease of above 10 ppbv, and could effectively prevent O$_3$ formation in the southweastern BTH region. The transportation emission reductions could effectively cut down O$_3$ concentrations in Beijing.

Electronic Supplementary Material: Supplementary material (the monthly H$_2$O$_2$/HNO$_3$ ratios Figs. S1–S5) is available online at http://dx.doi.org/10.1007/s00376-013-3132-x.

REFERENCES

An, J. L., Z. W. Han, Z. F. Wang, M. Y. Huang, S. W. Tao, and X. J. Cheng, 1999: Impacts of changes in the concentration of nonmethane hydrocarbon (NMHC) and NO$_x$ on amount of ozone formation. *Chinese J. Atmos. Sci.*, **23**(6), 753–761. (in Chinese)

An, J. L., Y. S. Wang, F. K. Wu, and B. Zhu, 2012a: Characterizations of volatile organic compounds during high ozone episodes in Beijing, China. *Environmental Monitoring and Assessment*, **184**, 1879–1889.

An, J. L, J. Li, W. Zhang, Y. Chen, Y. Qu, and W. L. Xiang, 2012b: Simulation of transboundary transport fluxes of air pollutants among Beijing, Tianjin, and Hebei Province of China. *Acta Scientiae Circumstantiae*, **32**(11), 2684–2692. (in Chinese)

Beijing Bureau of Statistics, 2007: Beijing Statistics Yearbook 2007. China Statistics Press, Beijing. (in Chinese)

Cai, H., and S. D. Xie, 2011: Traffic-related air pollution modeling during the 2008 Beijing Olympic Games: The effects of an odd-even day traffic restriction scheme. *Science of the Total Environment*, **409**, 1935–1948.

Castell, N., E. Mantilla, A. F. Stein, R. Salvador, and M. Millán, 2011: Simulation and evaluation of control strategies for ozone reduction in a complex terrain in southwestern Spain. *Environmental Modeling & Assessment*, **16**, 565–576.

Chan, C. K., and X. H. Yao, 2008: Air pollution in mega cities in China. *Atmos. Environ.*, **42**, 1–42.

Chou, C. C. K., C.-Y. Tsai, C.-J. Shiu, S. C. Liu, and T. Zhu, 2009: Measurement of NO$_y$ during campaign of air quality research in Beijing 2006 (CARE Beijing-2006): Implications for the ozone production efficiency of NO$_x$. *J. Geophys. Res.*, **114**, D00G01, doi: 10.1029/2008JD010446.

Cohan, D. S., A. Hakami, Y. T. Hu, and A. G. Russell, 2005: Non-linear response of ozone to emissions: Source apportionment and sensitivity analysis. *Environ. Sci. Technol.*, **39**, 6739–6748.

Diem, J. E., 2000: Comparisons of weekday-weekend ozone: importance of biogenic volatile organic compound emissions in the semi-arid southwest USA. *Atmos. Environ.*, **34**, 3445–3451.

Duan, J. C., J. H. Tan, L. Yang, S. Wu, and J. M. Hao, 2008: Concentration, sources and ozone formation potential of volatile organic compounds (VOCs) during ozone episode in Beijing. *Atmospheric Research*, **88**, 25–35.

Dudhia, J., 1989: Numerical study of convection observed during the winter monsoon experiment using a mesoscale two-dimensional model. *J. Atmos. Sci.*, **46**, 3077–3107.

Emmons, L. K., and Coauthors, 2010: Description and evaluation of the Model for Ozone and Related chemical Tracers, version 4 (MOZART-4). *Geoscientific Model Development*, **3**, 43–67.

ENVIRON, 2011: User's guide. Comprehensive air quality model with extensions version 5. 40. ENVIRON International Corporation, Novato, California. [Available online at http://www.camx.com.]

Gao, Y., and M. G. Zhang, 2012: Sensitivity analysis of surface ozone to emission controls in Beijing and its neighboring area during the 2008 Olympic Games. *Journal of Environmental Sciences*, **24**, 50–61.

Guenther, A., and Coauthors, 1995: A global model of natural volatile organic compound emissions. *J. Geophys. Res.*, **100**, 8873–8892.

Guenther, A., T. Karl, P. Harley, C. Wiedinmyer, P. I. Palmer, and C. Geron, 2006: Estimates of global terrestrial isoprene emissions using MEGAN (Model of Emissions of Gases and Aerosols from Nature). *Atmospheric Chemistry & Physics Discussions*, **6**, 107–173.

Guttikunda, S. K., and Coauthors, 2005: Impacts of Asian megacity emissions on regional air quality during spring 2001. *J. Geophys. Res.*, **110**, D20301, doi:10.1029/2004JD004921.

Han, Z. W., H. Ueda, and K. Matsuda, 2005: Model study of the impact of biogenic emission on regional ozone and the effectiveness of emission reduction scenarios over eastern China. *Tellus B*, **57**, 12–27.

Hao, J. M., D. Q. He, Y. Wu, L. X. Fu, and K. B. He, 2000: A study of the emission and concentration distribution of vehicular pollutants in the urban area of Beijing. *Atmos. Environ.*, **34**, 453–465.

Harris, L. M., and D. R. Durran, 2010: An idealized comparison of one-way and two-way grid nesting. *Mon. Wea. Rev.*, **138**, 2174–2187.

He, S. Z., and Coauthors, 2010: Measurement of atmospheric hydrogen peroxide and organic peroxides in Beijing before and during the 2008 Olympic Games: Chemical and physical factors influencing their concentrations. *J. Geophys. Res.*, **115**, D17307, doi: 10.1029/2009JD013544.

IPCC, 2001: *Climate Change* 2001*: The Scientific Basis. Contribution of Working Group I to the Third Assessment Report of the Intergovernmental Panel on Climate Change*, Houghton et al., Eds., Cambridge Univ. Press, New York, USA, 881 pp.

Hong, S. Y., and H. L. Pan, 1986: Nonlocal boundary layer vertical diffusion in a medium range forecast model. *Mon. Wea. Rev.*, **124**, 2322–2339.

Huang, Q., S. Y. Cheng, J. B. Li, D. S. Chen, H. Y. Wang, and X. R. Guo, 2012: Assessment of PM10 emission sources for

priority regulation in Urban air quality management using a new coupled MM5-CAMx-PSAT modeling approach. *Environmental Engineering Science*, **29**, 343–349.

Jiang, W. H., and J. Z. Ma, 2006: Implementation of NO_x and O_3 key source tracing method in a regional chemical transport model. *Acta Meteorologica Sinica*, **64**, 281–292. (in Chinese)

Kain, J. S., and J. M. Fritsch, 1993: Convective parameterization for mesoscale models: The Kain-Fritsch scheme. The representation of cumulus convection in numerical models. *Meteor. Monogr.*, **24**, 165–170.

Li, Y., A. H. Lau, J. C.-H. Fung, J. Y. Zheng, L. J. Zhong, and P. K. K. Louie, 2012: Ozone source apportionment (OSAT) to differentiate local regional and super-regional source contributions in the Pearl River Delta region, China. *J. Geophys. Res.*, **117**(D15305), doi: 10.1029/2011JD017340.

Lin, X., M. Trainer, and S. C. Liu, 1988: On the nonlinearity of the tropospheric ozone production. *J. Geophys. Res.*, **93**, 15 879–15 888.

Liu, F., Y. G. Zhu, and Y. Zhao, 2008: Contribution of motor vehicle emissions to surface ozone in urban areas: A case study in Beijing. *International Journal of Sustainable Development and World Ecology*, **15**, 345–349.

Ma, J., and J. A. van Aardenne, 2004: Impact of different emission inventories on simulated tropospheric ozone over China: A regional chemical transport model evaluation. *Atmos. Chem. Phys.*, **4**, 877–887.

Ma, J. Z., and Coauthors, 2012: The IPAC-NC field campaign: a pollution and oxidization pool in the lower atmosphere over Huabei, China. *Atmos. Chem. Phys*, **12**, 3883–3908.

McKeen, S. A., E.-Y. Hsie, and S. C. Liu, 1991: A study of the dependence of rural ozone on ozone precursors in the eastern United States. *J. Geophys. Res.*, **96**, 15 377–15 394.

Misenis, C., and Y. Zhang, 2010: An examination of sensitivity of WRF/Chem predictions to physical parameterizations, horizontal grid spacing, and nesting options. *Atmospheric Research*, **97**, 315–334.

Mlawer, E. J., S. J. Taubman, P. D. Brown, M. J. Iacono, and S. A. Clough, 1997: Radiative transfer for inhomogeneous atmospheres: RRTM, a validated correlated-k model for the longwave. *J. Geophys. Res.*, **102**, 16 663–16 682.

NARSTO, 2000: An assessment of tropospheric ozone pollution–A North American perspective. The NARSTO Synthesis Team, Palo Alto, CA. [Available online at http://www.narsto.org/sites/narsto-dev.ornl.gov/files/Chapter1.pdf.]

Peng, Y. P., K.-S. Chen, H.-K. Wang, C.-H. Lai, M.-H. Lin, and C.-H. Lee, 2011: Applying model simulation and photochemical indicators to evaluate ozone sensitivity in southern Taiwan. *Journal of Environmental Sciences*, **23**, 790–797.

Qu, Y., and J. L. An, 2009: Total and synergistic impacts of anthropogenic and biogenic emissions on ozone–Examples in East Asia in spring and summer. *China Environmental Science*, **29**(3), 337–344.

Qu, Y., J. L. An, H. Zhou, and X. F. Ye, 2009: Synergistic impacts of anthropogenic and biogenic emissions on spring surface ozone in East Asia. *Chinese J. Atmos. Sci.*, **33**(4), 670–680.

Qu, Y., J. L. An, and J. Li, 2013: Synergistic impacts of anthropogenic and biogenic emissions on summer surface O_3 in East Asia. *Journal of Environmental Sciences*, **25**(3), 520–530.

Shao, M., M. P. Zhao, Y. H. Zhang, L. X. Peng, and J. L. Li, 2000: Biogenic VOCs emissions and its impact on ozone formation in major cities of China. *Journal of Environmental Science and Health (A)*, **35**, 1941–1950.

Shao, M., S. H. Lu, Y. Liu, X. Xie, C. C. Chang, S. Huang, and Z. M. Chen, 2009: Volatile organic compounds measured in summer in Beijing and their role in ground-level ozone formation. *J. Geophys. Res.*, **114**, D00G06, doi: 10.1029/2008jd010863.

Shao, M., B. Wang, S. H. Lu, B. Yuan, and M. Wang, 2011: Effects of Beijing Olympics control measures on reducing reactive hydrocarbon species. *Environ. Sci. Technol.*, **45**, 514–519.

Shen, J., X. S. Wang, J. F. Li, Y. P. Li, and Y. H. Zhang, 2011: Evaluation and intercomparison of ozone simulations by Models-3/CMAQ and CAMx over the Pearl River Delta. *Science China*: *Chemistry*, **54**, 1789–1800.

Song, Y., M. Shao, Y. Liu, S. H. Lu, W. Kuster, P. Goldan, and S. D. Xie, 2007: Source apportionment of ambient volatile organic compounds in Beijing. *Environ. Sci. Technol.*, **41**, 4348–4353.

Stein, U., and P. Alpert, 1993: Factor separation in numerical simulations. *J. Atmos. Sci.*, **50**, 2107–2115.

Streets, D. G., and Coauthors, 2003: An inventory of gaseous and primary aerosol emissions in Asia in the year 2000. *J. Geophys. Res.*, **108**(D21), 8809, doi: 10.1029/2002jd003093.

Streets, D. G., and Coauthors, 2007: Air quality during the 2008 Beijing Olympic Games. *Atmos. Environ.*, **41**, 480–492.

Tang, G., Y. Wang, X. Li, D. Ji, S. Hsu, and X. Gao, 2012: Spatial-temporal variations in surface ozone in Northern China as observed during 2009–2010 and possible implications for future air quality control strategies. *Atmos. Chem. Phys.*, **12**, 2757–2776.

Tang, X., Z. F. Wang, J. Zhu, A. E. Gbaguidi, Q. Z. Wu, J. Li, and T. Zhu, 2010: Sensitivity of ozone to precursor emissions in urban Beijing with a Monte Carlo scheme. *Atmos. Environ.*, **44**, 3833–3842.

Tao, Z. N., S. M. Larson, D. J. Wuebbles, A. Williams, and M. Caughey, 2003: A summer simulation of biogenic contributions to ground-level ozone over the continental United States. *J. Geophys. Res.*, **108**(D14), 4404, doi: 10.1029/2002 JD002945.

Tao, Z. N., S. M. Larson, A. Williams, M. Caughey, and D. J. Wuebbles, 2005: Area, mobile, and point source contributions to ground level ozone: a summer simulation across the continental USA. *Atmos. Environ.*, **39**, 1869–1877.

Thunis, P., and C. Cuvelier, 2000: Impact of biogenic emissions on ozone formation in the Mediterranean area-a BEMA modelling study. *Atmos. Environ.*, **34**, 467–481.

The United Nations Environment Program (UNEP), 2009: *Independent Environmental Assessment: Beijing* 2008 *Olympic Games*. The United Nations Environment Program, 139pp.

Wang, S. X., and Coauthors, 2010a: Quantifying the air pollutants emission reduction during the 2008 Olympic Games in Beijing. *Environ. Sci. Technol.*, **44**, 2490–2496.

Wang, T., and S. D. Xie, 2009: Assessment of traffic-related air pollution in the urban streets before and during the 2008 Beijing Olympic Games traffic control period. *Atmos. Environ.*, **43**, 5682–5690.

Wang, T., and Coauthors, 2010b: Air quality during the 2008 Beijing Olympics: Secondary pollutants and regional impact. *Atmos. Chem. Phys.*, **10**, 7603–7615.

Wang, X. M., G. Carmichael, D. L. Chen, Y. H. Tang, and T. J. Wang, 2005: Impacts of different emission sources on air quality during March 2001 in the Pearl River Delta (PRD) region. *Atmos. Environ.*, **39**, 5227–5241.

Wang, X. S., and J. L. Li, 2002: The effect of anthropogenic hydrocarbons to ozone formation in Beijing areas. *Environ. Sci.*

Technol., **22**, 22–26 (in Chinese).

Wang, Y. X., J. Hao, M. B. McElroy, J. W. Munger, H. Ma, D. Chen, and C. P. Nielsen, 2009a: Ozone air quality during the 2008 Beijing Olympics: effectiveness of emission restrictions. *Atmos. Chem. Phys.*, **9**, 5237–5251.

Wang, X. S., J. L. Li, Y. H. Zhang, S. D. Xie, and X. Y. Tang, 2009b: Ozone source attribution during a severe photochemical smog episode in Beijing, China. *Science in China* (*B*), **52**, 1270–1280.

Weinroth, E., M. Luria, C. Emery, A. Ben-Nun, R. Bornstein, J. Kaplan, M. Peleg, and Y. Mahrer, 2008: Simulations of Mideast transboundary ozone transport: A source apportionment case study. *Atmos. Environ.*, **42**, 3700–3716.

World Health Organization (WHO), 2004: Ethics in Health research. [Available online at http://whqlibdoc.who.int/emro/2004/9290213639_chap2.pdf.]

Wu, Q. Z., Z. F. Wang, H. S. Chen, W. Zhou, and M. Wenig, 2012: An evaluation of air quality modeling over the Pearl River Delta during November 2006. *Meteorology and Atmospheric Physics*, **116**, 113–132.

Wu, Y., D. S. Ji, T. Song, B. Zhu, and Y. S. Wang, 2011: Characteristics of atmospheric pollutants in Beijing, Zhuozhou, Baoding and Shijiazhuang during the period of summer and autumn. *Environmental Science*, **32**, 2741–2749. (in Chinese)

Xin, J. Y., and Coauthors, 2010: Variability and reduction of atmospheric pollutants in Beijing and its surrounding area during the Beijing 2008 Olympic Games. *Chinese Science Bulletin*, **55**, 1937–1944.

Xing, J., and Coauthors, 2011: Modeling study on the air quality impacts from emission reductions and atypical meteorological conditions during the 2008 Beijing Olympics. *Atmos.*

Environ., **45**, 1786–1798.

Yang, Q., Y. H. Wang, C. Zhao, Z. Liu, W. I. Gustafson, Jr., and M. Shao, 2011: NO$_x$ emission reduction and its effects on ozone during the 2008 Olympic Games. *Environ. Sci. Technol.*, **45**, 6404–6410.

Yarwood, G., S. Rao, M. Tocke, and G. Z. Whitten, 2005: Updates to the Carbon Bond Mechanism: CB05. ENVIRON International Corporation, Novato. Report to the U. S. Environmental Protection Agency. [Available online at http://www.camx.com/publ/pdfs/CB05_Final_Report_120805.pdf.]

Yuan, Z. B., A. K. H. Lau, M. Shao, P. K. K. Louie, S. C. Liu, and T. Zhu, 2009: Source analysis of volatile organic compounds by positive matrix factorization in urban and rural environments in Beijing. *J. Geophys. Res.*, **114**, D00G15, doi: 10.1029/2008jd011190.

Zhang, H. L., and Coauthors, 2012: Source apportionment of PM$_{2.5}$ nitrate and sulfate in China using a source-oriented chemical transport model. *Atmos. Environ.*, **62**, 228–242.

Zhang, J., Z. Y. Ouyang, H. Miao, and X. K. Wang, 2011: Ambient air quality trends and driving factor analysis in Beijing, 1983–2007. *Journal of Environmental Sciences*, **23**, 2019–2028.

Zhang, L., J. R. Brook, and R. Vet, 2003: A revised parameterization for gaseous dry deposition in air-quality models. *Atmos. Chem. Phys.*, **3**, 2067–2082.

Zhang, Q., and Coauthors, 2009: Asian emissions in 2006 for the NASA INTEX-B mission. *Atmos. Chem. Phys.*, **9**, 5131–5153.

Zhu, B., J. L. An, Z. F. Wang, and Y. Li, 2006: Relations of diurnal variations of photochemical ozone to its precursors. *Journal of Nanjing Institute of Meteorology*, **29**, 744–749. (in Chinese)